APPLIED PHYSICS LETTERS

Effect of anharmonicity of the strain energy on band offsets in semiconductor nanostructures

Olga L. Lazarenkova, ^{a)} Paul von Allmen, Fabiano Oyafuso, and Seungwon Lee *Jet Propulsion Laboratory, California Institute of Technology, Pasadena, California 91109*

Gerhard Klimeck

Jet Propulsion Laboratory, California Institute of Technology, Pasadena, California and Network for Computational Nanotechnology, School of Electrical and Computer Engineering, Purdue University, West Lafayette, Indiana 47906

(Received 25 May 2004; accepted 7 September 2004)

Anharmonicity of the interatomic potential is taken into account for the quantitative simulation of the conduction and valence band offsets for strained semiconductor heterostructures. The anharmonicity leads to a weaker compressive hydrostatic strain than that obtained with the commonly used quasiharmonic approximation of the Keating model. Compared to experiment, inclusion of the anharmonicity in the simulation of strained InAs/GaAs nanostructures results in an improvement of the electron band offset computed on an atomistic level by up to 100 meV. © 2004 American Institute of Physics. [DOI: 10.1063/1.1814810]

The accurate simulation of the electronic structure is of utmost importance for the design of nanoelectronic and optoelectronic device structures. It has been shown both theoretically 1,2 and experimentally, 1,3-5 that the energy spectrum in semiconductor nanostructures is extremely sensitive to the built-in strain. The continuum elasticity method fails to adequately describe the strain profile in InAs/GaAs heterostructures with a 7% lattice mismatch between the constituent materials. The two-parameter valence-force-field (VFF) Keating model 6,7 is a commonly used approximation for atomistic-level calculations of the equilibrium atomic positions in realistic-size nanostructures. In this letter the quasiharmonic Keating model is shown to be insufficient to describe highly strained InAs/GaAs nanostructures due to the anharmonicity of the strain energy.

The Keating model treats atoms as spring-connected points in a crystal lattice. The strain energy depends only on nearest-neighbor interactions^{6,7}

$$E = \frac{3}{8} \sum_{m} \left\{ \sum_{n} \left[\frac{\alpha_{mn}}{d_{mn}^{2}} (\mathbf{r}_{mn} \cdot \mathbf{r}_{mn} - \mathbf{d}_{mn} \cdot \mathbf{d}_{mn})^{2} + \sum_{k \geq n} \frac{\sqrt{\beta_{mn} \beta_{mk}}}{d_{mn} d_{mk}} (\mathbf{r}_{mn} \cdot \mathbf{r}_{mk} - \mathbf{d}_{mn} \cdot \mathbf{d}_{mk})^{2} \right] \right\}.$$
(1)

The coefficient α corresponds to the spring constant for the bond length distortion, while β corresponds to the change of the angle between the bonds ("bond-bending"). The summation is over all atoms m of the crystal and their nearest neighbors n and k. \mathbf{r}_{mn} and \mathbf{d}_{mn} are the vectors connecting the mth atom with its nth neighbor in the strained and unstrained material, respectively.

The Keating potential in Fig. 1 (dashed line) fails to reproduce the weakening of the realistic interatomic interaction (solid line with circles) with increasing distance between atoms and it underestimates the repulsive forces at close atomic separation. Therefore Eq. (1) can adequately describe the strain energy only at small deformations. In InAs/GaAs

The anharmonicity is included directly into the VFF constants α and β of the Keating model

$$\alpha_{mn} = \alpha_0^{mn} \left[1 - A_{mn} \frac{(r_{mn}^2 - d_{mn}^2)}{d_{mn}^2} \right], \tag{2}$$

$$\beta_{mnk} = \beta_0^{nmk} \left[1 - B_{nmk} (\cos \theta^{nmk} - \cos \theta_0^{nmk}) \right]$$

$$\times \left[1 - C_{nmk} \frac{(r_{mn}r_{mk} - d_{mn}d_{mk})}{d_{mn}d_{mk}} \right],$$
(3)

with $\beta_0^{nmk} \equiv \sqrt{\beta_0^{mn}\beta_0^{mk}}$, $B_{nmk} \equiv \sqrt{B_{mn}B_{mk}}$, and $C_{nmk} \equiv \sqrt{C_{mn}C_{mk}}$. θ^{nmk} and θ_0^{nmk} are the actual and the unstrained angles between mn and mk bonds, respectively. In homogeneous materials all bonds are the same and the indexes m, n, and k can be dropped. α_0 and β_0 are the VFF constants in the unstrained crystal. The anharmonicity corrections A and C describe the dependence of α and β on hydrostatic strain, while B is responsible for the change of the bond-bending term with the angle between bonds. The details of the derivation of A, B, and C from the experimental phonon spectra of

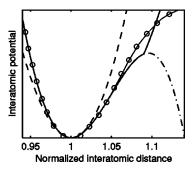


FIG. 1. Schematic interatomic potential used in the Keating (dashed line) and our model (solid line). Dash-dot line plots the potential with the anharmonicity corrections to the VFF constants before the truncation. The line marked with large circles approximatly traces the shape of the realistic potential.

heterostructures, the lattice mismatch is as large as 7% and anharmonicity of the interatomic potential is expected to become important.

a)Electronic mail: olga.l.lazarenkova@jpl.nasa.gov

4194

TABLE I. Valence-force-field constants in unstrained materials and anharmonicity corrections for InAs and GaAs.

Material	$\alpha_0({ m N/m})$	$\beta_0(N/m)$	A	В	С
GaAs	41.49	8.94	7.2	7.62	6.4
InAs	35.18	5.49	7.61	4.78	6.45

strained bulk materials are presented in Ref. 9. The parameters used for the simulation are listed in Table I.

The introduction of the anharmonicity corrections in the VFF model makes the form of the potential more realistic and expands the range of validity of the strain simulations. In order to ensure the convergence of the minimization of the strain energy (1) with α and β given by Eqs. (2) and (3), our model interatomic potential (dash-dot line in Fig. 1) is truncated (solid line in Fig. 1).

To illustrate the effect of the anharmonicity on the strain distribution in III–V semiconductor nanostructures, the hydrostatic, $\epsilon_H = 1/3(\epsilon_{xx} + \epsilon_{yy} + \epsilon_{zz})$, and biaxial, $\epsilon_B = 1/6(\epsilon_{xx} + \epsilon_{yy} - 2\epsilon_{zz})$, components of the strain in InAs/GaAs single (SQW) and multiple quantum well and in GaAs/InAs single quantum barrier (SQB) have been computed using both the conventional Keating model and our model (Table II). Comparing the results of the two models, we note that the sharp rise of the strain energy at small interatomic distances leads to a smaller equilibrium hydrostatic compression than is obtained with the Keating model. The bond stretching is underestimated in the quasiharmonic approximation. The biaxial compression is increased in our anharmonic model, while the biaxial tension is suppressed.

The band offsets for InAs/GaAs nanostructures obtained for the strain distribution simulated within the Keating and anharmonic models are compared with the available experimental data^{3–5} in Table III. The local band structure was obtained within the $sp^3d^5s^*$ empirical tight-binding model where the Hamiltonian matrix elements depend on the distance between the atoms. The tight-binding parameters¹⁰ were fitted to reproduce the properties of the strained bulk materials.¹¹ The discrepancy between the experimental and simulated energies is significantly smaller in the anharmonic model (see Table III).

The strain distribution [Figs. 2(a) and 2(b)] and the energy spectrum [Fig. 2(c)] were computed for the quantum dot crystal (QDC) reported in Ref. 5. The structure consists of three layers of *regimented* vertically stacked dome-shaped quantum dot arrays (with a 20 nm base diameter and a 7 nm height) on top of the 0.7 nm wetting layer, with a small (3 nm) vertical separation between the QD layers. The built-in strain distribution in such structures is very inhomogeneous. The average hydrostatic component of the strain

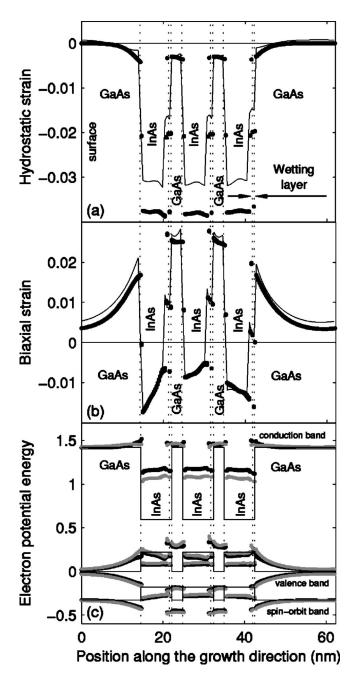


FIG. 2. Computed distribution of the hydrostatic (a) and biaxial (b) strain components, and (c) electronic band structure along the growth direction in the InAs/GaAs QDC structure taken from Ref. 5. The cross section is made near the center of the quantum dot stack. The results obtained with the Keating model are plotted with black dots. The results obtained with the anharmonic model are plotted with solid line on (a) and (b) and with gray dots on (c). The thin lines on (c) show the edges of conduction, valence, and spin-orbit split-off bands at the center of the Brillouin zone in the unstrained materials.

TABLE II. Hydrostatic (H) and biaxial (B) strain components with the x epitaxial layer in different epitaxial nanostructures computed within the Keating (K) and anharmonic (A) model. L_x is the width of the x layer, L_y is the width of the y layer (thickness of the capping layer for SQW and SQB), $\delta(\%) = 100(\epsilon^K - e^A)/\epsilon^A$.

Ref.	Composition		Structure	Size		Substr.	Hydrostatic strain (%)			Biaxial strain (%)		
	x	у		L_x	$L_{\rm y}$		$\epsilon_{\!\scriptscriptstyle H}^{\scriptscriptstyle K}$	$oldsymbol{\epsilon}_{H}^{A}$	δ_H	ϵ_B^K	ϵ_{B}^{A}	δ_{B}
3	InAs	GaAs	SQW	2 ML	5 ML	GaAs	-2.97	-2.59	14.9	-3.71	-4.10	-9.4
3	GaAs	InAs	SQB	2 ML	5 ML	InAs	3.54	4.30	-17.7	3.72	2.90	28.3
4	InAs	GaAs	MQW	1 ML	30 nm	GaAs	-2.87	-2.33	23.5	-3.81	-4.38	-13.0

TABLE III. Experimental band offsets in the conduction (ΔE_c) and valence (ΔE_v) bands compared with the offsets computed within the $sp^3d^5s^*$ empirical tight-binding model using the equilibrium atomic positions found within the two-parameter Keating model (K) and including anharmonicity corrections to the VFF constants (A) for 2 ML InAs/GaAs SQW and GaAs/InAs SQB 5 ML away from the surface, MQW formed by 1 ML InAs separated by 30 nm GaAs layers and InAs/GaAs QDC consisting of three vertically separated on about 3 nm layers of dome-shaped QDs with a 20 nm base and a 7 nm height on top of a 0.7 nm wetting layer. The band offsets are determined so they would be positive for potential well and negative for potential barrier. *Notations*: XPS—x-ray photoemission spectroscopy, CV—capacitance-voltage spectroscopy, DLTS—deep-level transient spectroscopy, hh—heavy hole, lh—light hole. δ_K and δ_A estimate the relative deviations of the simulation from the experiment.

Ref.	Structure	Experimental		$\Delta E_c({ m meV})$					$\Delta E_v({ m meV})$					
		method	K	$\delta_{\it K}(\%)$	A	$\delta_{\!A}(\%)$	Exp.	K	$\delta_{\it K}(\%)$	A	$\delta_{\!A}(\%)$	Exp.	Subband	
3	SQW	XPS	471.5		574.0			374.6	-34.4	447.0	-15.7	530±50	hh	
3	SQB	XPS	-40.7		-91.3			-271.7	69.8	-225.9	41.2	-160 ± 50	lh	
4	MQW	CV&DLTS	475.7	-31.1	584.4	-15.3	690	373.4		430.5			hh	
5	QDC	DLTS	242.0	-29.0	347.0	1.8	$341\!\pm\!30$							

tensor inside InAs quantum dots [Fig. 2(a)] is overestimated by about 25% within the commonly used Keating model. The biaxial strain distribution [Fig. 2(b)] changes little when computed with the different models.

The main effect of the anharmonicity is a downward shift of the conduction band edge inside the quantum dots [Fig. 2(c)]. This is caused by the sensitivity of the conduction band to the hydrostatic compression, which is smaller within the anharmonic model. The difference in the corresponding band edges obtained within the two models is as large as 105.0 meV. This shift brings the overall band offset between the InAs quantum dot and GaAs buffer computed in our model very close to the experimentally observed value (see Table III). Due to the small difference in the biaxial strain distribution obtained with the two models [Fig. 2(b)], the energy structure of the valence band remains almost the same [Fig. 2(c)].

In conclusion, it is demonstrated that the anharmonicity is important for the modeling of the electronic states in strained InAs/GaAs systems. Compared to the standard Keating model corrections of over 100 meV are found in some band offsets, resulting in values significantly closer to the experimental data. This demonstrates that the deformation in the nanostructures is beyond the range of applicability of the quasiharmonic approximation for the strain energy. The anharmonicity corrections can be performed without a significant increase of the computational cost, since the model remains limited to the nearest neighbour interactions.

This work has been done at the Jet Propulsion Laboratory, California Institute of Technology under a contract with the National Aeronautics and Space Administration. Funding was provided under grants from ARDA, ONR, JPL, NASA, and NSF (Grant No. EEC-0228390). This work was performed while one of the authors (O.L.L.) held a National Research Council Research Associateship Award at JPL.

Shumway, A. J. Williamson, A. Zunger, A. Passaseo, M. DeGiorgi, R. Cingolani, M. Catalano, and P. Crozier, Phys. Rev. B 64, 125302 (2001).
 C. Pryor, J. Kim, L. W. Wang, A. J. Williamson, and A. Zunger, J. Appl. Phys. 83, 2548 (1998).

³K. Hirakawa, Y. Hashimoto, K. Harada, and T. Ikoma, Phys. Rev. B 44, 1734 (1991).

⁴R. Colombelli, V. Piazza, A. Badolato, M. Lazzarino, F. Beltram, W. Schoenfeld, and P. Petroff, Appl. Phys. Lett. **76**, 1146 (2000).

⁵S. Ghosh, B. Kochman, J. Singh, and P. Bhattacharya, Appl. Phys. Lett. **76**, 2571 (2000).

⁶P. N. Keating, Phys. Rev. **145**, 637 (1966).

⁷R. M. Martin, Phys. Rev. B **1**, 4005 (1970).

⁸L.-W. Wang, J. Kim, and A. Zunger, Phys. Rev. B **59**, 5678 (1999).

⁹O. L. Lazarenkova, P. von Allmen, F. Oyafuso, S. Lee, and G. Klimeck (unpublished).

¹⁰F. Oyafuso, G. Klimeck, P. von Allmen, T. Boykin, and R. C. Bowen, Phys. Status Solidi B 239, 71 (2003).

We used the parameter set from Ref. 10 corresponding to the commonly used positive valence band hydrostatic deformation potential a_v. Use of the small negative a_v suggested by S.-H. Wei and A. Zunger, Phys. Rev. B 60, 5404 (1999) shifts the valence band energies up in the compressed InAs/GaAs structures, bringing the simulation closer to the experiment, while the downward shift of the valence band in stretched GaAs/InAs structures leads to the larger deviation from the experiment. For the 3% hydrostatic strain the energy shift is about 0.18 eV.